Method for Direct Measurement of Structural Rolling Resistance for Heavy Vehicles

Nielsen, Natasja Ringsing; Chatti, Karim ; Nielsen , Christoffer; Zaabar, Imen; Hjorth, Poul G. ; Hecksher, Tina

Published in:
Transportation Research Record

DOI:
10.1177/0361198120915699

Publication date:
2020

Document Version
Peer reviewed version

Citation for published version (APA):
Nielsen, N. R., Chatti, K., Nielsen , C., Zaabar, I., Hjorth, P. G., & Hecksher, T. (2020). Method for Direct Measurement of Structural Rolling Resistance for Heavy Vehicles. *Transportation Research Record*, *2674*(5), 371-380. https://doi.org/10.1177/0361198120915699

Method for Direct Measurement of Structural Rolling Resistance for Heavy Vehicles

Natasja R. Nielsen, Corresponding Author
Roskilde University
Universitetsvej 1, 4000 Roskilde, Denmark
Email: narini@ruc.dk

Karim Chatti
Department of Civil and Environmental Engineering, Michigan State University,
428 S. Shaw Lane, Room 3546, East Lansing, MI 48824-1226, USA
Email: chatti@egr.msu.edu

Christoffer P. Nielsen
Greenwood Engineering A/S
H. J. Holst Vej 3-5C, 2605 Brøndby, Denmark
Email: christoffer@greenwood.dk

Imen Zaabar
Department of Computer Science and Engineering, Michigan State University,
428 S. Shaw Lane, Room 3546, East Lansing, MI 48824-1226, USA.
Email: zaabarim@egr.msu.edu

Poul G. Hjorth
DTU Compute
Richard Petersens Plads, Bygning 324, 2800 Kgs. Lyngby, Denmark
Email: pghj@dtu.dk

Tina Hecksher
Roskilde University
Universitetsvej 1, 4000 Roskilde, Denmark
Email: tihe@ruc.dk

Word Count: 5000 words + 5 table(s) $\times$ 250 = 6250 words

Submission Date: October 12, 2020

ABSTRACT

In this paper, a new in-situ method for determining the structural rolling resistance (SRR) defined as the dissipated energy due to deformation of the pavement when subjected to a moving load, is presented. The method is based on the relation between structural rolling resistance and the slope of the deflection basin under a moving load. Using the Traffic Speed Deflectometer, the deflection slope is measured at several positions behind and in front of the right rear-end tire pair of a full-size truck trailer while driving under realistic conditions. The deflection slope directly under the tire is estimated from a linear interpolation between the two nearest sensors. A set of data from a test road segment located in Denmark is analysed and the SRR coefficients were found to be in the range 0.005-0.05 %.

The deflection slope measurements have a high reproducibility (repeated measurements agree within standard deviations of 4-10 %) with high spatial resolution, and the method for calculating SRR from these measurements has the clear advantage that it requires no knowledge or model of the pavement structure or viscoelastic properties. Numerical simulations of pavement response show that the proposed interpolation method tends to underestimate the actual SRR, and better estimates can be obtained by other interpolation schemes.

Keywords: structural rolling resistance, moving load, deflection slope measurements, asphalt pavement, Traffic Speed Deflectometer

INTRODUCTION

When driving at constant speed, the fuel consumption goes into overcoming driving resistance. Many different factors contribute to the driving resistance in a vehicle; among the most prominent are uphill driving, air drag, internal friction and rolling resistance (*1*). It is estimated that for heavy trucks, 15-30 % of the fossil fuel input is used to overcome the rolling resistance (*2*). Rolling resistance losses arise from two main sources: 1) viscoelastic effects in the tires and 2) effects of the pavement, including unevenness, texture, and viscoelastic deformation of the pavement (*3–5*). The focus in this paper is on the latter.

An elastic or viscoelastic pavement subject to a moving vehicle will deform underneath the tires. If the pavement is viscoelastic, this deformation will result in energy dissipating into the pavement structure. The lost energy has to be compensated through additional work from the vehicle engine, in order to maintain a constant driving speed (*6*). The amount of additional energy needed depends on the structure of the pavement and we will refer to this as structural rolling resistance (SRR) throughout the paper.

The deflection basin under a moving tire is asymmetric due to viscoelastic properties of the pavement causing a time delay in the deflection of a viscoelastic pavement. This time delay makes the maximum deflection appear behind the center of the tire, as seen on Figure 1a. This means that the tire always will be on an uphill slope, see Figure 1b, and thus has to do work in order to maintain a constant driving speed (*7*). Using this uphill slope notion, the SRR can be calculated directly from the asymmetric deflection basin (*1, 8, 9*). Deflection of a structure subject to a moving load has been reported in the literature since the 1960's, e.g. in Flügge (*7*), where the viscoelastic response of a Kelvin beam is analyzed, and the viscoelastic effects reported to manifest themselves through an asymmetric deflection basin.

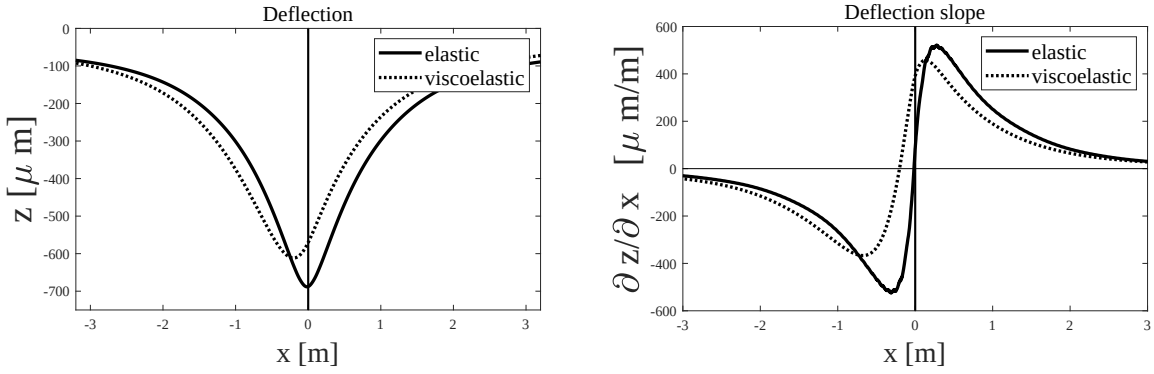

(a) (b)

FIGURE 1: **(a) Simulated deflection basin underneath a moving load for an elastic (solid line) and viscoelastic (dotted line) pavement. The basin is obtained using a numerical simulation explained at a later point in this paper. (b) Associated deflection slope for the elastic and viscoelastic pavement. Due to the symmetric deflection basin for the elastic pavement,** $\frac{\partial z(x=0)}{\partial x} = 0$**, whereas the asymmetry in the viscoelastic deflection basin makes** $\frac{\partial z(x=0)}{\partial x} > 0$**.**

While structural rolling resistance has been studied for decades, it has proven difficult to devise accurate and robust ways of measuring the SRR. As a consequence, little is known about the absolute magnitude of SRR or its relative contribution to the overall rolling resistance. Indirect

measurements of the influence of the dissipative effects in bituminous layers have been estimated by comparing fuel consumption measurements on flexible and rigid pavements. These studies rely on the assumption that rigid pavements have little or no viscous losses and thus the difference in fuel consumption between these types of pavements can be ascribed to the viscous behavior of the asphalt (*8, 10, 11*). However, it can be difficult to isolate the effects that relates to the pavement structure, from other effects due to, e.g., texture or unevenness (*9*). Also, unlike texture and unevenness, the effect from pavement structure is found to be highly dependent on external parameters such as temperature, pavement conditions, etc. (*12*). It is therefore difficult to say anything conclusive on SRR influence on fuel consumption based on these types of experiments.

Direct estimates of SRR typically come from simulations of pavement deflections with pavement parameters obtained either from backcalculations using falling weight deflectometer tests or other rhelogical measurements of the bituminous layer. An often used method is to simulate the pavement response in a finite pavement section, as a moving load is passing with constant speed (*13*). From the response, one can obtain the displacement field of the pavement surface and calculate the dissipated energy in the pavement (*3, 11, 14–16*). On the basis of such calculations, it is believed that the SRR loss is smaller than the energy loss due to pavement texture and unevenness (*14*), but whether it is negligible or significant enough that it should be included in pavement planning is not clear.

Development of methods for reliable measurement of the pavements influence on the vehicle fuel consumption, is thus highly desired when making lifecycle assessment studies on pavements and should be included in the development of sustainable pavement designs (*3, 6*).

In this paper, we present a novel method for determining the structural rolling resistance under realistic driving conditions using the Traffic Speed Deflectometer technology developed by Greenwood Engineering. The technique measures the slope of the deflection basin between the right pair of rear-end tires of a full-size truck trailer, as it moves at realistic driving speeds. Thus, the uphill slope seen by the tire due to the deformation of the pavement is directly measured and from this, the associated SRR loss can be calculated. The estimated SRR is thus obtained under conditions directly comparable to what normal traffic experiences. The method gives spatially resolved (10 m resolution), reproducible and robust estimates of SRR, even in road segments where the value fluctuates considerably, making it a reliable and model-free method to measure structural rolling resistance.

AIM

We present a new concept for measuring structural rolling resistance using Traffic Speed Deflectometer (TSD) technology. The TSD measures the slope of the deflection basin under the tires of a truck trailer during driving. The concept and its robustness is demonstrated by pilot measurements of a test road segment of nine kilometers and the assumptions behind are discussed in the light of numerical pavement simulations.

THE TRAFFIC SPEED DEFLECTOMETER CONCEPT

The Traffic Speed Deflectometer (TSD) is conventionally used for continuous bearing capacity measurements by evaluating the slope of the pavement deflection basin. It has the advantage that it makes continuous measurements of the the deflection slope and that the TSD trailer is a normal truck trailer and thus can measure under normal driving speed and load as well as measuring directly in the wheel path. In this study a full axle load of 10 tonnes was used.

The TSD device measures the deflection velocity of the pavement as it is subjected to a moving load. This is done by use of Doppler lasers, that measure the vertical velocity of the pavement. The TSD truck is equipped with 9 Doppler lasers (sensors): 3 sensors located behind and 6 in front of the rear-end axle, see Figure 2a. Their exact positions relative to the center of the axle (in meters) are

$$\text{Sensor position} = [-0.366, -0.269, -0.167, 0.163, 0.260, 0.362, 0.662, 0.964, 1.559]\,. \tag{1}$$

The measured pavement velocity is adjusted such that effects due to vertical movements of the truck is subtracted. This is done by using a reference laser mounted 3.1 meters from the rear-end axle, where the deflection of the pavement is assumed zero (red sensor on Figure 2a). The technique is explained in more detail in (*17–20*).

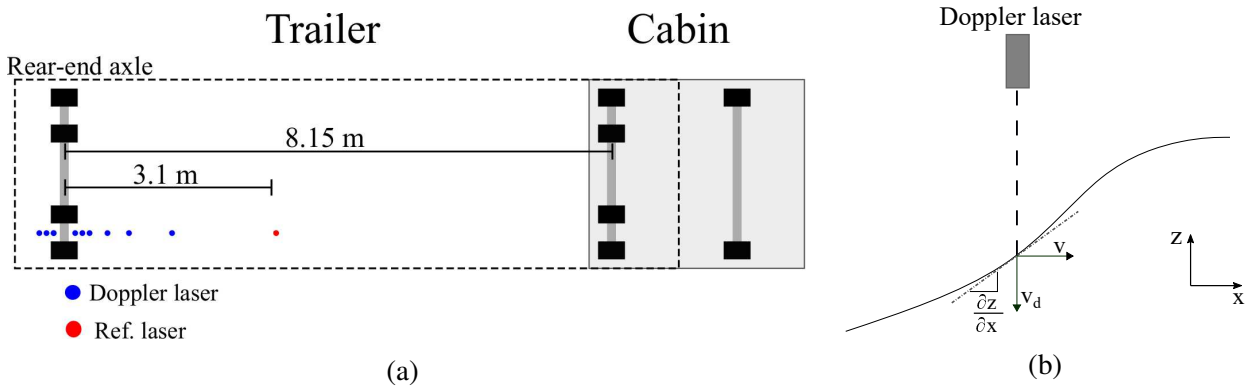

FIGURE 2: **(a) Top view sketch of the TSD. Nine Doppler lasers (sensors) are located in between the right rear-end tire pair indicated with blue dots. The measured vertical pavement velocity is adjusted for vertical movement of the truck due to, e.g., unevenness in the road, by a reference sensor located 3.1 m from the rear-end axle and indicated with a red dot. Note that the drawing is not to scale, and the tires in the tire-pairs are only separated by 64 mm. (b) The vertical pavement velocity (v_d) in a given point is measured using a Doppler laser. The deflection slope in that point ($\frac{\partial z}{\partial x}$) corresponds to the slope of the tangent going through the point (grey dotted line) and can be found by dividing $v_d$with the horizontal driving speed, v.**

The slope of the deflection basin at the sensor point can be found by dividing the measured vertical pavement velocity (v_d) with the driving speed (v)

$$\frac{\partial z}{\partial x} = \frac{\frac{\partial z}{\partial t}}{\frac{\partial x}{\partial t}} = \frac{v_d}{v}\,, \tag{2}$$

as is illustrated in Figure 2b. The driving speed, v, is measured using a odometer located behind the right rear-end tire pair.

DEFLECTION SLOPE DATA

For this study, we made 3 repeated measurements on the same road with the TSD. The measurements were conducted on a 9.7 km road section near Copenhagen, Denmark, in the spring of 2018 with almost constant air temperature ($\sim 14°$C) and road temperature ($\sim 18°$C) throughout all three measurements. The driving speed was between 50-60 km/h; the exact driving speed was recorded continuously during all measurements. The measured deflection slopes for each sensor were collected at a sampling frequency of 1000 samples pr. second, and was later averaged over 10 m. A plot of the mean value for the three subsequent measurements of each sensor as a function of the driven distance is seen on Figure 3. Clearly, the measured deflection slope for each sensor varies significantly throughout the measured distance. This variation is however completely reproducible with average standard deviations between 12-26 μm/m (corresponding to 4-10 %) between the three measurement runs.

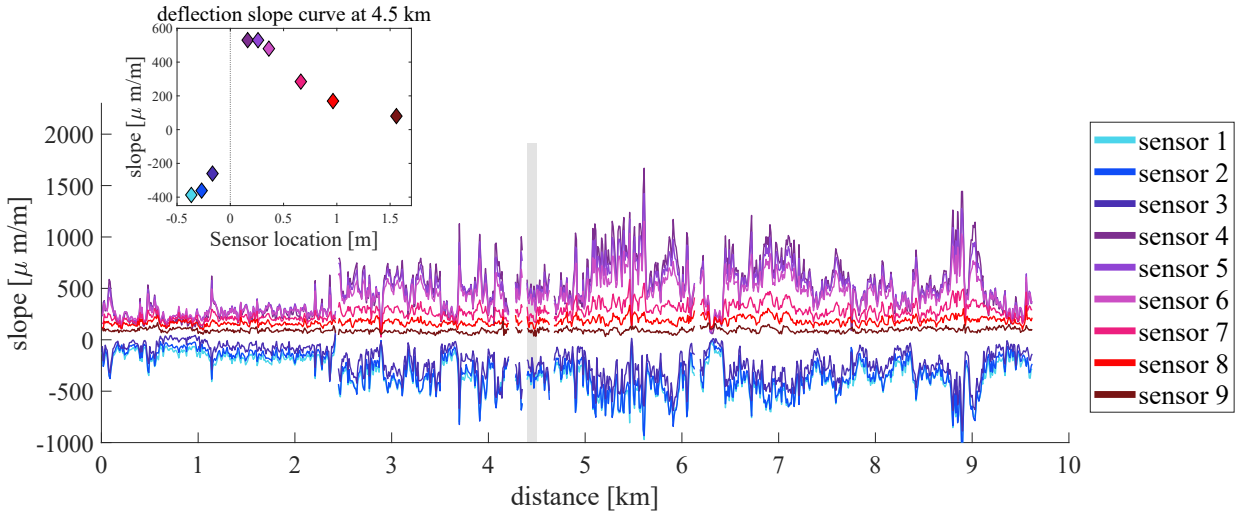

FIGURE 3: **Measured deflection slope for each sensor as a function of the distance. The inset shows a plot of the deflection slopes measured at 4.5 km (marked with gray) as a function of the sensor loaction. The center of the axle is marked with a dotted line in $x = 0$.**

The inset in Figure 3 shows measured deflection slope as a function of the sensor position measured at 4.5 km. The center of the axle in this plot is at $x = 0$ indicated with a black dotted line. As mentioned in the introduction, the deflection slope curve is characterized by the minimum deflection slope occurring behind and the maximum deflection slope in front of the tire. The asymmetry in minimum and maximum peak magnitudes is believed to be caused by damping in the pavement. Thus the location and magnitude of the maximum and minimum carries information about the visco-elastic properties of the pavement.

For analysis of the data, we need to estimate the deflection slope at the axle location, i.e., around $x = 0$, where we can not measure due to the presence of the axle. Instead, we need to infer the slope from the measured locations in front of and behind the center position. This task

is easier when the features of the deflection slope are fully captured by the sensors, which is not the case for all traces. Accordingly, we partitioned the measurements into 3 groups based on the behavior of the signal in sensor 4,5,6 (table 1), which gives an indication of where the maximum is located: group 1 for measurements where the maximum is not captured by the sensors and hence must be located closer to the center of the axle than sensor 4, group 2 for measurements where the maximum is partly captured by the sensors, and group 3 for measurements where the maximum is fully captured by the sensors, see table 1. Examples of measurements from each group are shown on Figure 4a. Within group 1 and 2 we found a big variation in the magnitude of the maximum and the minimum, while for measurements belonging to group 3 this variation was not observed.

TABLE 1: **Partitioning of the TSD measurements into groups. The division is made based on the behavior of the measured deflection slope in sensor 4,5 and 6. In total this gives 3 groups which is illustrated on Figure 4a.**

	group 1	group 2	group 3
Behaviour of signal in sensor 4, 5 and 6	monotonic decreasing	increasing or equal from sensor 4 to 5 and then decreasing in sensor 6	monotonic increasing
Location of maximum	closer to center of axle than sensor 4	partly captured by sensor 4 and 5	fully captured by the sensors

CALCULATING THE STRUCTURAL ROLLING RESISTANCE

We now show how the structural rolling resistance (SRR) loss can be calculated directly from the measured deflection slope data.

In the following we assume that the applied load is a point load at the center of the tire, corresponding to $x = 0$ and with the magnitude F_L. The dissipated power due to SRR, P_{SRR}, can be found from the applied load and the pavement velocity at this point,

$$P_{SRR} = F_L v_d(x=0) = F_L v \frac{\partial z}{\partial x}(x=0)\,, \tag{3}$$

where the last equality sign comes from Equation (2).

In the case of a perfectly elastic pavement, the maximum deflection will occur directly under the load, making the deflection slope at this point zero and thus $P_{SRR} = 0$. For a viscoelastic pavement, however, the maximum deflection occurs behind the load and there is an uphill slope underneath the load, thus $P_{SRR} > 0$, as already illustrated in Figure 1. Note that, the deflection maximum occurs behind the center of the load whether we consider a point load or a finite contact area. Thus the tire also experiences an up-hill slope if considered a finite contact area, and thereby has $P_{SRR} > 0$ whenever there is damping in the pavement.

To estimate the deflection slope directly under the tire, we use a linear interpolation between the measured deflection slope in the two sensors located closest to the center (sensor 3 and 4), located at $x = -0.167$ m and $x = 0.163$ m respectively, see Figure 4b. Hence the dissipated energy

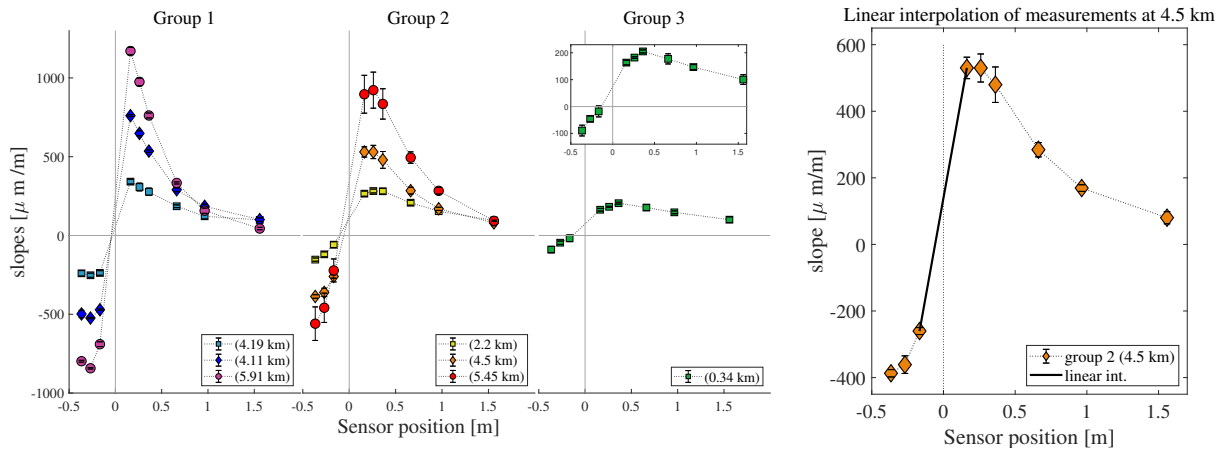

(a) (b)

FIGURE 4: **(a) The measured TSD data is divided into 3 groups based on how much of the deflection slope maximum is captured by sensors 4, 5, and 6 (see table 1). We show examples of deflection slope plotted as a function of the sensor location for the different groups. (b) Linear interpolation between the measured values in the two sensors closest to the axle for data measured after 4.5 km belonging to group 2. The symbols are the average values of the three repeated measurements and the errorbars represent the standard deviations, showing a high degree of reproducibility.**

can be written as follows

$$P_{SRR} = F_L v b\,, \tag{4}$$

where b is the intersection of the linear interpolation $\frac{\partial z}{\partial x}(x) = ax + b$ with the z-axis, $\frac{\partial z}{\partial x}(x = 0)$. From the dissipated power we can define the rolling resistance force as $F_{SRR} = \frac{P_{srr}}{v} = F_L b$. Using the standard definition of rolling resistance coefficient as the ratio between rolling resistance force and the load, this leads to the following simple relation between deflection slope at $x = 0$ and the SRR coefficient

$$C_{SRR} = \frac{F_{SRR}}{F_L} = b\,. \tag{5}$$

Using these relations on the data trace presented in Figure 4b, we find an SRR power of 49 W $\pm$ 6 W, an SRR force of 6.8 N $\pm$ 0.8 N and $C_{SRR} = 1.4 \cdot 10^{-4} \pm 1.6 \cdot 10^{-5}$ or 0.014% $\pm$ 0.0016%

The C_{SRR} value for all measurement sets were found following this procedure, and the results are presented in Figure 5. Here, the symbols represent the mean values of the three repeated measurements and the errorbars are found as the standard deviation of the three measurements. We see that the C_{SRR} value varies considerably over the travelled distance, from 0.005-0.05 % with most data points in the region from 0.01-0.02 %. The method shows a good reproducibility with low standard deviations, even in regions where the C_{SRR} changes rapidly with distance. This demonstrates that the method is robust and can measure the C_{SRR} values of the road precisely with high spatial resolution even under changing pavement conditions.

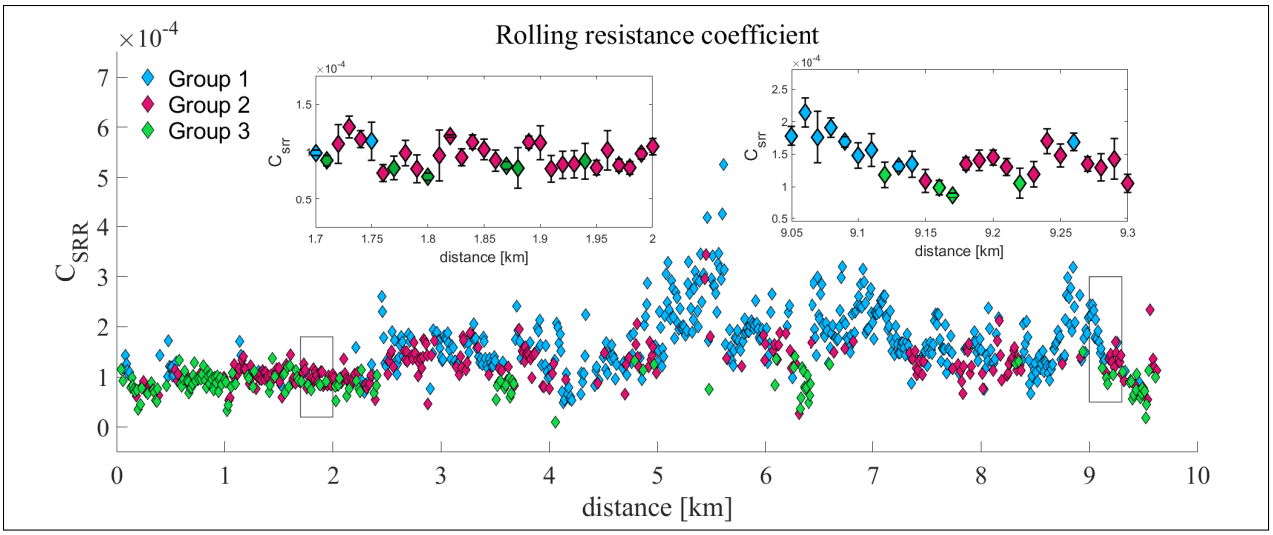

FIGURE 5: **Calculated C_{SRR} values plotted versus distance. The different groups are marked with different colors. We see that the values vary over the measured road segment, reflecting a change in the deflection slope curve. Zoom in is made of a steady and a varying section and the standard deviations are illustrated by errorbars. We see low standard deviations in both areas, illustrating the robustness of the method.**

The different data groups are indicated with red, green and blue on figure 5. Average values of P_{SRR} , F_{SRR} and C_{SRR} for each group is shown in table 2. The groups were divided based on the location of the maximum, captured by sensor 4,5,6, and we see a clear difference in the SRR values within the different groups. Furthermore, the variations in C_{SRR} with distance seen in Figure 5 follow the trends seen in the measured deflection slopes in Figure 3. This is due to the fact that a large deflection slope signal in the sensors closest to the axle (sensor 3 and 4) generally results in a high intersection value with the y axis, and thus a high calculated C_{SRR} (Equation (5)).

The magnitude and the location of the peaks in the deflection slope curves, are determined by the shape of the deflection basin, which mainly is controlled by the relative stiffness of the top asphalt layer compared to the lower layers. For situations with a relative stiff top layer, the deflection basin will be broad and have a small amplitude, resulting in curves like group 3 and a small SRR. Whereas a relative soft top layer will give a deep and narrow basin, giving deflection curves like group 1 and a higher SRR. This is consistent with what we see in the measurements.

TABLE 2: **Average C_{SRR} F_{SRR} and P_{SRR} for the three groups of TSD data. We see that SRR for data in group 1 is largest, followed by group 2 and then group 3. The number af measurements within the dataset belonging to each group is listed in the last column.**

	P_{SRR} [Watt]	F_{SRR} [N]	C_{SRR}	# in group
group 1	124.2 ± 57.2	8.6 ± 3.0	$1.7 \cdot 10^{-4} \pm 6 \cdot 10^{-5}$	506
group 2	84.9 ± 30	5.9 ± 1.8	$1.2 \cdot 10^{-4} \pm 4 \cdot 10^{-5}$	272
group 3	61.7 ± 21	4.2 ± 1.3	$0.9 \cdot 10^{-4} \pm 3 \cdot 10^{-5}$	159

IMPACT OF A FINITE CONTACT SURFACE

For the calculations of the dissipated power and C_{SRR} above, we assumed that the interaction between tire and road can be described as a point load. This is a simplification of the real interaction between the tire and the pavement where the contact surface has a finite area. To investigate whether this approximation has a significant influence on the calculated SRR loss, we adopt an expression for the power dissipation derived by Chupin et al. (*9*). The expression is based on a moving reference frame with constant velocity, which is consistent with the TSD setup. Furthermore, it is assumed that the tire is elastic and hence does not dissipate energy and that the tire provides a uniform applied stress to the surface,

$$P_{SRR}^{contact\ area} = pv \int_S \frac{\partial z(X,y,z)}{\partial X} dS. \tag{6}$$

Here, p is the tire pressure, v is the driving speed, z is the vertical component of the displacement field of the pavement surface, and $\frac{\partial z(X,y,z)}{\partial X}$ is the deflection slope. The integral is taken over the contact surface, S, which is the area where the tire is in contact with the pavement. Plugging in a linearly varying deflection slope and assuming a circular contact area we obtain

$$\begin{aligned} P_{SRR}^{contact\ area} &= pv \int_S \frac{\partial z(X,y,z)}{\partial X} dS = pv \int_{-r}^{r} \int_{-\sqrt{r^2-X^2}}^{\sqrt{r^2-X^2}} (aX+b)\, dy\, dX \\ &= pvb\pi r^2 = Fvb = P_{srr}^{point\ load}. \end{aligned} \tag{7}$$

Thus, for a linearly varying deflection slope the power dissipated over a finite contact area is equal to the power dissipated at a point load.

MODEL CALCULATION OF PAVEMENT RESPONSE

So far, we have assumed that the deflection slope underneath the tire is linearly varying and can be found by interpolation between the two sensors near the axle. We will now investigate the validity of this assumption by use of simulated deflection slopes. The purpose of this is solely to generate curves with similar behaviors to those observed in the measurements, and to investigate how well the assumption of a linear deflection slope performs for the simulated curves. In particular, this is not an attempt to model the exact pavement response measured, but rather a theoretical exploration of the interpolation approach.

For simulating the pavement response, we use the time-domain based viscoelastic solver ViscoWave II-M, developed at Michigan State University (*21, 22*). Viscowave II-M employs the so-called spectral element method to solve the wave propagation problem in the pavement structure and calculate the pavement response to an arbitrary loading. The model can simulate the time-dependent responses and allows each pavement layer to be either elastic or viscoelastic (*23*).

The program was modified slightly for this study such that the simulated conditions are similar to the TSD set-up and hence can be used for comparison. The original solver calculates the pavement deflection under the tire in a steady reference frame. The modified version calculates the response between the two tires in the tire reference frame, i.e., a moving reference frame. From the simulated deflection curve the corresponding slope was calculated and filtered to remove numerical noise.

The pavement structure used for the simulation consists of 3 layers, representing an asphalt

TABLE 3: **(a) Mechanical characteristics for the simulated pavement. All pavement structures are made of three layers, each characterized by their Poisson's ratio (ν), mass density (ρ), average thickness (h) and the relaxation modulus (E). The relaxation modulus for the asphalt layer is given by Equation** (8)**.**

Asphalt
E(t)
$\nu = 0.35$
$\rho = 2322.7\ \frac{\text{kg}}{\text{m}^3}$
$h = 0.15$ m
Base
$E_2 = 124.3$ MPa
$\nu = 0.35$
$\rho = 2082.4\ \frac{\text{kg}}{\text{m}^3}$
$h = 0.3$ m
Subgrade
$E_3 = 65.4$ MPa
$\nu = 0.45$
$\rho = 1762\ \frac{\text{kg}}{\text{m}^3}$
$h = \infty$

layer, a base layer, and a subgrade layer. We simulated four different pavement models with identical contruction only changing visco-elastic parameters for the asphalt (top) layer. The parameters for the structure (height, elastic moduli, Poisson's ratio and density) are chosen to be typical values for these kinds of pavement layers and they are listed in table 3. The viscoelastic properties of the asphalt layer are described by the relaxation modulus $E(t)$, given by

$$\log(E(t)) = c_1 + \frac{c_2}{1 + e^{(-c_3 - c_4 \log(t_R))}}, \tag{8}$$

$$\log(t_R) = \log(t) - \log(a_T)\,, \tag{9}$$

where $c_1, \ldots, c_4$ are the sigmoid coefficients, t_R is the reduced time and a_T is the shift factor (*16*).

The parameters for the relaxation moduli are taken from backcalculated falling weight deflectometer tests on road segments located in California, in order to have realistic $E(t)$ curves (*16*). The characteristics of these moduli range from very stiff with high damping to very soft with little damping, see table 4. These sets of parameters generated deflection slope curves with a similar variation to that seen in the data groups as shown in Figure 6a. In the simulated deflection curves, the stiff pavement with large damping (PAV4) shows a small deflection and deflection slope peaks far apart, whereas the soft pavement with little damping (PAV1) has the opposite behavior. Probably, other choices of pavement parameters could result in similar deflection basin. However, for the present purpose the detailed input parameters of the model are not so important, as long as they are reasonably realistic.

In Figure 6b a zoom of the contact region for each of the simulated deflection slope curves

TABLE 4: **For the study, four different E(t) were used and their properties are listed here.**

	Pavements			
	PAV1	PAV2	PAV3	PAV4
Sigmoid coefficients				
c_1	1.4	1.054	0.978	1.67
c_2	2.04	2.986	3.8	3.39
c_3	0.944	0.335	0.521	0.981
c_4	-0.417	-0.436	-0.519	-0.767
Shift factor $\log(a_T)$	0.37	0.32	0.49	0.34
E(t) characteristics				
E_0 [Mpa]	2,753	10,956	59,970	114,820
$E_0 - E_\infty$ [Mpa]	2,728	10,945	59,960	114,770
Stiffness	⟶			
Amount of damping	⟶			

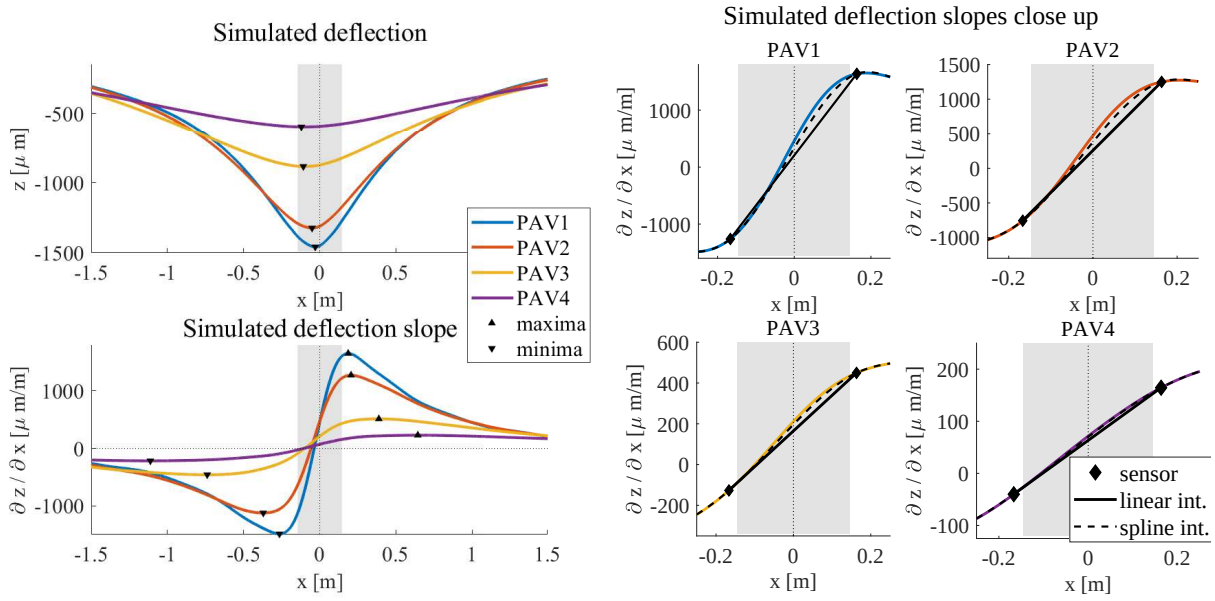

FIGURE 6: **(a) Simulated deflection and deflection slope curves for four pavements with different $E(t)$ of the asphalt layer. (b) Close up of the simulated deflection slope curves. The contact area between the tire and pavement is assumed circular with radius (r). The interval [-r;r] is marked with a gray color. A linear and a cubic spline interpolation between the positions of the two sensors closest to the axle in the experiment is marked with a black and a dotted line respectivly.**

is shown. We want to determine how much the *actual* SRR in the simulated deflection slope curve deviates from the SRR obtained by assuming a linear interpolation between coordinates of the two sensors closest to the axle in the measurement. The linear interpolation is marked on Figure 6b by a black line and the SRR is found as the intersection of this linear interpolation with the z-axis.

For calculating the SRR for the simulations we integrate the deflection slope over the contact area as described above in Equation (6). Again assuming a circular contact area with origin in $x = 0$ and radius r. We use $r = 14.5$ cm, found from the tire load and pressure of the TSD.

In addition to the linear interpolation, we have also made a cubic spline interpolation. In this, a 3rd order polynomial is used to find the values in between the two interpolation points instead of a linear function, and thus this gives a smoother interpolation curve. As this method has more unknown parameters to fit than the linear, we are using nine simulation points, corresponding with the coordinates of the TSD sensors, to make the interpolation. The spline interpolation is marked on Figure 6b with a dotted line. The spline interpolation is included in an attempt to approximate the actual deflection slope in the contact area better.

The relative difference between the interpolations and the simulation curves are found by the relative difference in the dissipated energy over the contact area,

$$\frac{\Delta P^{int.}}{P} = \frac{\int_S \frac{\partial z^{sim}}{\partial x} dS - \int_S \frac{\partial z^{int.}}{\partial x} dS}{\int_S \frac{\partial z^{sim}}{\partial x} dS}. \tag{10}$$

The calculated P_{SRR} values for the different deflection slope curves and the two interpolated curves are listed in table 5 along with their relative differences.

TABLE 5: **Calculated change in P_{SRR} of the simulated deflection slope and the linear and cubic spline interpolations for different pavements. Values for the calculated P_{SRR} of both the simulation and the interpolations are also shown for each pavement.**

Pavement	P_{srr}^{sim} [watt]	P_{srr}^{linear} [watt]	P_{srr}^{spline} [watt]	$\frac{\Delta P^{linear}}{P}$	$\frac{\Delta P^{spline}}{P}$
PAV1	335	172	257	49%	23%
PAV2	356	220	297	38%	17%
PAV3	170	134	159	17%	6%
PAV4	59	54	58	9%	2%

The analysis shows that the difference between the simulated deflection slope and the linear interpolation is small for PAV4, $\frac{\Delta P^{linear}}{P} = 9\%$, where the deflection maximum and minimum are far apart. With decreasing stiffness, and thus smaller distance between maximum and minimum, the error increase, with the largest deviation found in PAV1, where $\frac{\Delta P^{linear}}{P} = 49\%$.

The spline interpolation shows the same trend, but it gives a better estimate of SRR. Thus, for the PAV1 the difference is only $\frac{\Delta P^{spline}}{P} = 23\%$ while for PAV4 it gives pratically the same value as the model curve.

We can conclude that the linear assumption is valid when the deflection slope peaks are far apart, whereas it underestimates SRR, when the peaks are too close to the origin to be resolved. The

spline interpolation in all cases gives a slightly better estimate of SRR, especially for pavements where the peaks are close together.

Lastly, we employed the numerical calculations to estimate the difference in the deflection slope obtained underneath the tires and at the location of the TSD sensors. In the TSD set-up, the sensors are located between the tire pair (see Figure 2a) and hence the deflection slopes reported in this paper are measured in-between the tire pair. This deviates from the the analysis assumptions about the contact area in Equation 6, where it is assumed to be circular with origin in x=0. By simulating the pavement deflection for pavement PAV1 directly underneath the tires and in-between the tire pair respectively, it was found that the difference in P_{SRR} is 3.6%. Consequently, this does not have a significant impact on the final SRR results.

SUMMARY AND OUTLOOK

In this paper, we have presented a model-free way to estimate structural rolling resistance (SRR) from pavement deflection slope measurements obtained with the Traffic Speed Deflectometer (TSD). In the simplest approach, we assume the contact between tire and road is point-like (i.e., a "moving point load"). In that case, the SRR coefficient, C_{SRR}, is simply given as the value of the deflection slope curve at the position of the point load. Since it is not possible to measure exactly at that position due to the presence of the axle, the deflection slope was estimated from a linear interpolation of nearby measurement points behind and in front of that location. The point load assumption is shown to be equivalent to calculations based on a finite contact area, if the deflection slope varies linearly within the contact region.

A set of data from a test road was investigated and the values of C_{SRR} found by this method span from 0.005-0.05 %, which are modest values compared to typical rolling resistance coefficients of tires that are in the range 0.5-1 %. The values are slightly lower than those found in empirical and numerical studies on the subject (*9, 10, 14, 15*). The data were divided into three groups based on how much of the deflection slope maximum was resolved by the TSD sensors. This was based on the hypothesis that this criterion is critical for the linear interpolation to be a good estimate of the deflection slope under the tire. It was found that for measurements in group 1 with maximum located closes to the load, the SRR was highest and for group 3 with maximum located the furthest away, the SRR was lowest. Through simulated deflection slope curves obtained using the program ViscoWave II-M the linear interpolation was found to underestimate the actual SRR by up to $\sim$50% in the worst case. Using a cubic spline interpolation between nine positions corresponding to the TSD sensor positions, improved the SRR estimate considerably. Confirming that the resolution of the maximum is critical for the linear interpolation approach to give accurate results. Further development of the interpolation method will improve the method and improve the accuracy of the estimated SRR values. By use of numerical studies we aim to develop a simple functional expression that will allow the deflection slope values underneath the axle to be estimated with greater accuracy.

The strength of the method is that it requires no knowledge about the pavement structure or pavement properties. Furthermore, the use of the TSD vehicle makes data collection relatively fast and easy and the deflection slope measurements are very precise. This leads to reproducible values of C_{SRR} determined with low standard deviation, even in areas of the road where the values vary considerably.

The measurements included in this study were made on a test road with the purpose of illustrating the new method and was chosen for purely practical reasons. They were performed

in relatively cold conditions (pavement temp. $\sim 18^{\circ}$C) and a future study with higher pavement and air temperature is expected to provide higher SRR values. In the study, we found that the magnitude and location of the maximum deflection slope is correlated with the SRR. It is expected that these quantities are mainly dependent on the relative stiffness of the top layer compared with the underlying layers. Furthermore, the location of the maximum deflection depends on the amount of damping in the pavement (damping in top layer, foundation or a combination). The relationship between these pavement characteristics and the behaviour of the deflection slope curve should be explored further by use of simple physical models.
Through this new easy method for measuring SRR, it will be feasible to conduct a series of tests on roads with different pavement structures and thus investigate the relationship between pavement structure and SRR. Furthermore, the impact of road temperature or driving speed could also be investigated. Such large scale systematic surveys could provide much needed clarity in the study of SRR, and establish under which circumstances SRR is important for the overall fuel consumption as well as how it is affected by various parameters.

AUTHOR CONTRIBUTIONS

The authors confirm contribution to the paper as follows:
study conception and design: Natasja R. Nielsen, Christoffer P. Nielsen, Tina Hecksher, Poul G. Hjorth;
data collection: Christoffer P. Nielsen;
analysis and interpretation of results: Natasja R. Nielsen, Christoffer P. Nielsen, Imen Zaabar, Karim Chatti ;
draft manuscript preparation: Natasja R. Nielsen, Christoffer P. Nielsen, Tina Hecksher, Poul G. Hjorth, Karim Chatti, Imen Zaabar
All authors reviewed the results and approved the final version of the manuscript

REFERENCES

1. Chupin, O., J.-M. Piau, and A. Chabot, Effect of Bituminous Pavement Structures on the Rolling Resistance. In *11th International Conference On Asphalt Pavements*, 2010, pp. pp.1287–1296.
2. Hall, D. E. and J. C. Moreland, Fundamentals of rolling resistance. *Rubber Chemistry and Technology*, Vol. 74, No. 3, 2001, pp. 525–539.
3. Coleri, E. and J. T. Harvey, Impact of Pavement Structural Response on Vehicle Fuel Consumption. *Journal of Transportation Engineering, part B: pavements*, Vol. 143, No. 1, 2017.
4. Louhghalam, A., M. Akbarian, and F.-J. Ulm, Scaling Relationships of Dissipation-Induced Pavement-Vehicle Interactions. *Transportation Research Record: Journal of the Transportation Research Board*, Vol. 2457, 2014, pp. 95–104.
5. Bazi, G., E. Y. Hajj, A. Ulloa-Calderon, and P. Ullidtz, Finite element modelling of the rolling resistance due to pavement deformation. *International Journal of Pavement Engineering*, 2018, pp. 1–11.
6. Louhghalam, A., M. Akbarian, and F.-J. Ulm, Scaling Relationships of Dissipation-Induced Pavement-Vehicle Interactions. *Transportation Research Record: Journal of the Transportation Research Board*, Vol. 2457, No. 1, 2015, pp. 95–104.
7. Flügge, W., *Viscoelasticity*. Springer, Berlin, Heidelberg, 1975.
8. Balzarini, D., I. Zaabar, and K. Chatti, Effect of Pavement Structural Response on Rolling Resistance and Fuel Economy using a Mechanistic Approach. *Advances in Materials and Pavement Performance Prediction*, Vol. 10, 2018, pp. 49–51.
9. Chupin, O., J. M. Piau, and A. Chabot, Evaluation of the structure-induced rolling resistance (SRR) for pavements including viscoelastic material layers. *Materials and Structures/Materiaux et Constructions*, Vol. 46, No. 4, 2013, pp. 683–696.
10. Zaabar, I. and K. Chatti, A field investigation of the effect of pavement type on fuel consumption. In *T and Di Congress 2011 : Integrated Transportation and Development for a Better Tomorrow,*, 2014, pp. 772–781.
11. Balzarini, D., I. Zaabar, and K. Chatti, Impact of concrete pavement structural response on rolling resistance and vehicle fuel economy. *Transportation Research Record: Journal of the Transportation Research Board*, Vol. TRR 2640, No. 1, 2017, pp. 84–94.
12. Harvey, J. T., J. D. Lea, C. Kim, E. Coleri, I. Zaabar, A. Louhghalam, K. Chatti, J. Buscheck, and A. Butt, *Simulation of Cumulative Annual Impact of Pavement Structural Response on Vehicle Fuel Economy*. Univ. of California Pavement Research Center, Davis, CA., 2016.
13. Louhghalam, A., M. Akbarian, and F.-J. Ulm, Flügge's Conjecture: Dissipation- versus Deflection-Induced Pavement-Vehicle Interactions. *Journal of Engineering Mechanics*, Vol. 140, No. 8, 2013, p. 04014053.
14. Pouget, S., C. Sauzéat, H. D. Benedetto, and F. Olard, Viscous Energy Dissipation in Asphalt Pavement Structures and Implication for Vehicle Fuel Consumption. *Journal of Materials in Civil Engineering*, Vol. 24, No. 5, 2012, pp. 568–576.
15. Akbarian, M., S. S. Moeini-Ardakani, F. Ulm, and M. Nazzal, Mechanistic Approach to Pavement-Vehicle Interaction and Its Impact on Life-Cycle Assessment. *Transportation Research Record: Journal of the Transportation Research Board*, Vol. 2306, 2012, pp. 171–179.

16. Balzarini, D., K. Chatti, I. Zaabar, A. A. Butt, and J. T. Harvey, Mechanistic-Based Parametric Model for Predicting Rolling Resistance of Flexible Pavements. *Transportation Research Record: Journal of the Transportation Research Board*, Vol. 2673, No. 7, 2019, pp. 341–350.
17. Hildebrand, G. and S. Rasmussen, *Development of a High Speed Deflectograph*. Road Directorate, Danish Road Institute, 2002.
18. Krarup, J., S. Rasmussen, L. Aagaard, and P. G. Hjorth, *Output From the Greenwood Traffic Speed Deflectometer*, 2006.
19. Chai, G., S. Manoharan, A. Golding, G. Kelly, and S. Chowdhury, Evaluation of the Traffic Speed Deflectometer data using simplified deflection model. *Transportation Research Procedia*, Vol. 14, 2016, pp. 3031–3039.
20. Nielsen, C. P., Visco-Elastic Back-Calculation of Traffic Speed Deflectometer Measurements. *Transportation Research Record: Journal of the Transportation Research Board*, 2019, pp. 1–9.
21. Lee, H. S., *Development of a New Solution for Viscoelastic Wave Propagation of pavements structures and its use in dynamic backcalculations*. Ph.D. thesis, Michigan State University, 2013.
22. Balzarini, D., I. Zaabar, K. Chatti, and M. Losa, Impact of Flexible Pavement Structural Response on Rolling Resistance and Vehicle Fuel Consumption. In *World Conference on Pavement and Asset Management*, 2017.
23. Lee, H. S., H. V. Quintus, and D. Steel, Effect of moving dynamic loads on pavement deflections and backcalculated modulus. In *Proceedings of the TRB 97th Annual Meeting*, 2018.